High-pulse-energy, linear optical parametric oscillator with narrow and symmetrical far field

Øystein Farsund* **and Gunnar Rustad**

Norwegian Defence Research Establishment (FFI), PO Box 25, NO-2027 Kjeller, Norway
*Oystein.Farsund@ffi.no

Abstract: A new method to obtain a narrow and symmetrical far field from a high-pulse-energy optical parametric oscillator (OPO) with a linear resonator has been tested. The OPO employs two identical nonlinear crystals that are cut for type II phase matching, rotated such that their walk-off planes are orthogonal, and separated by a broadband half-wave plate. The OPO has a simple geometry, can be double-pass pumped, is wavelength tunable and operates stably with high conversion efficiency. The method has been demonstrated in a KTP-based OPO pumped at 1064 nm and a BBO-based OPO pumped at 532 nm, with output pulse energies up to 60 mJ and 75 mJ, respectively.

OCIS codes: (190.4410) Nonlinear optics, parametric processes; (190.4420) Nonlinear optics, transverse effects in; (190.4970) Parametric oscillators and amplifiers.

References and links

1. G. Rustad, G. Arisholm, and Ø. Farsund, "Effect of idler absorption in pulsed optical parametric oscillators," Opt. Express **19**(3), 2815–2830 (2011).
2. C. D. Nabors and G. Frangineas, "Optical parametric oscillator with bi-noncolinear, porro prism cavity," in Advanced Solid State Lasers, OSA Trends in Optics and Photonics, Vol. **10**, (Optical Society of America, Orlando, FL, 1997), 90–93.
3. A. V. Smith and M. S. Bowers, "Image-rotating cavity designs for improved beam quality in nanosecond optical parametric oscillators," J. Opt. Soc. Am. B **18**(5), 706–713 (2001).
4. D. J. Armstrong and A. V. Smith, "Demonstration of improved beam quality in an image-rotating optical parametric oscillator," Opt. Lett. **27**(1), 40–42 (2002).
5. O. Farsund, G. Arisholm, and G. Rustad, "Improved beam quality from a high energy optical parametric oscillator using crystals with orthogonal critical planes," Opt. Express **18**(9), 9229–9235 (2010).
6. W. J. Alford, R. J. Gehr, R. L. Schmitt, A. V. Smith, and G. Arisholm, "Beam tilt and angular dispersion in broad-bandwidth, nanosecond optical parametric oscillators," J. Opt. Soc. Am. B **16**(9), 1525–1532 (1999).
7. G. Arisholm, "General numerical methods for simulating second-order nonlinear interactions in birefringent media," J. Opt. Soc. Am. B **14**(10), 2543–2549 (1997).
8. G. Arisholm, "Advanced numerical simulation models for second-order nonlinear interactions," Proc. SPIE **3685**, 86–97 (1999).
9. D. Eimerl, L. Davis, S. Velsko, E. K. Graham, and A. Zalkin, "Optical, Mechanical, and Thermal-Properties of Barium Borate," J. Appl. Phys. **62**(5), 1968–1983 (1987).
10. D. J. Armstrong, W. J. Alford, T. D. Raymond, A. V. Smith, and M. S. Bowers, "Parametric amplification and oscillation with walkoff-compensating crystals," J. Opt. Soc. Am. B **14**(2), 460–474 (1997).
11. M. Kaucikas, M. Warren, A. Michailovas, R. Antanavicius, and J. J. van Thor, "Beam patterns in an optical parametric oscillator set-up employing walk-off compensating beta barium borate crystals," Laser Phys. **23**(2), 025401 (2013).

1. Introduction

Optical parametric oscillators (OPOs) provide a powerful and potentially efficient means of producing tunable coherent light. The quality of the beams generated by an OPO depends on the beam quality of the pump beam, the details of the resonator geometry and details of the nonlinear process. For low pulse energies, narrow beams can be used, and a properly designed resonator geometry may lead to excellent beam quality. However, in some applications, in particular within the field of remote sensing, high pulse energy in combination with high beam quality is required. This poses a substantial challenge as the beam then must be made relatively wide to avoid optical damage, and the resonator geometry is no longer able to ensure a high quality beam. We have previously shown that an OPO pumped with nanosecond pulses has potential for generating high beam quality provided that the diameter of the pump beam is smaller than the limit given by [1] $d_{\max} \approx \sqrt{2\tau_p c\lambda}$, where τ_p is the pump pulse length, c is the speed of light in vacuum and λ is the signal wavelength. For 5 ns pulses and 1.6 µm signal wavelength, this limit becomes ~2 mm. If the peak pump fluence is to be held below, say, 2 J/cm^2, this will limit the maximum pump energy for a Gaussian beam to ~35 mJ. For higher pulse energies (or lower damage thresholds), other means must therefore be used to ensure a good beam quality.

The divergence of the signal and idler beams can be restricted by choosing a nonlinear material and interaction with low angular acceptance for the signal. This occurs when there is spatial walk-off between signal and idler in the nonlinear material, as in type 2 collinear critical phase matching. For type 1 phase matching or for quasi-phase matching, this effect cannot be used for collinear phase matching, but is possible for non-collinear phase matching [2]. For OPOs with large beams, but small signal acceptance angle, the far field of the signal beam typically becomes asymmetric, with a narrow far field (and good beam quality) in the direction of signal-idler walk-off and a (much) wider far field in the other direction [3].

There exist several methods to mitigate this problem and create a symmetrical and narrow far field even from a large beam OPO. In the RISTRA ring resonator, the image of the signal beam (but not the polarization) is rotated 90° each round trip, building up spatial coherence in both directions [3, 4]. Nabors and Frangineas [2] used non-collinear pumping to generate signal-idler walk-off and a resonator with a porro-prism to flip the signal beam image. We have previously demonstrated good and symmetrical beam quality using two different type 2 phase matched crystals with orthogonal critical planes (OCP) in the same linear resonator using two-pass pumping [5]. While all approaches have succeeded in generating good beam qualities, they also have some limitations. The OCP requires two different crystals that match each other in terms of birefringence, nonlinearity and wavelength range. The porro-prism OPO cannot be angle tuned, while the RISTRA geometry require materials with relatively high nonlinear gain as the resonator round-trip path is fairly long and the pump cannot be double-passed through the nonlinear material.

Smith and Bowers proposed and simulated a number of approaches to achieve high beam quality from high energy, nanosecond OPOs [3], including the RISTRA. In this work, we demonstrate experimentally one of the other configurations they propose; two type 2 phase matched crystals with orthogonal critical planes in a standing wave cavity with an inter-crystal half-wave plate which rotates the pump and signal polarizations by 90°. This geometry resembles the OCP, but by introducing the half-wave plate, the need for different crystals in the OCP geometry is lifted. The OPO has a simple geometry and two pass pumping ensures a symmetric signal far field [3] as well as high efficiency. The OPO geometry was tested both with two KTP and with two BBO crystals, with 1064 nm and 532 nm pumping wavelength, respectively, at > 100 mJ pump energies.

2. Experiment

The linear OPO resonator was built as sketched in Fig. 1. The OPO was pumped with either the 1064 nm output from a Q-switched 10 Hz pulse-rate flash-lamp pumped Nd:YAG laser generating 5 ns multi longitudinal mode pulses with approximately 20 GHz linewidth (Quantel Brilliant B), or the frequency doubled output of the same laser. The pump energy could be adjusted from 0 to 270 mJ at 1064 nm (0 to 170 mJ at 532 nm) with a half-wave plate and a polarizer, and the pump beam diameter was varied from 3 mm to 7 mm by changing the lenses in the telescope. The input mirror was highly reflective on the signal wavelength, and had high transmission at the pump and idler wavelengths. Two different pairs of crystals were used, as listed in Table 1.

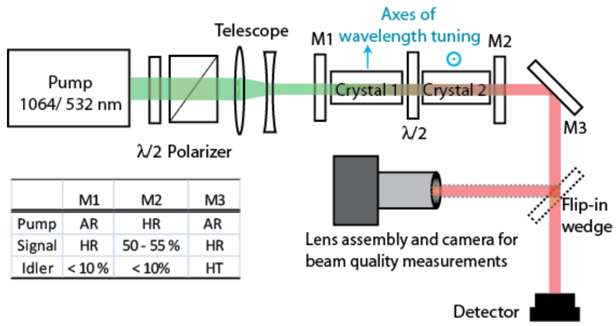

Fig. 1. Experimental setup and mirror specifications for the OPOs pumped by either 1064 nm or 532 nm.

Table 1. Nonlinear Crystals Used in the Experiments[a]

Crystal	Length	Cut angle	AR Pump/Signal
BBO	16 mm	23°	532/670
KTP	30 mm	46° (XZ)	1064/1680

[a]All crystals were cut for type 2 phase matching and used in pairs, and the AR-coating also had low loss on the corresponding idler wavelength. The cross sections of the crystals were 8 mm × 8 mm.

A commercial achromatic half-wave plate (Thorlabs AHWP05M-1600 for 1064 nm pump and AHWP05M-600 for 532 nm pump) was placed between the crystals and oriented to give 90° polarization rotation of the pump and signal beams. The output coupler reflected ~50% at the signal wavelength, < 10% at the idler wavelength and was highly reflective at the pump wavelength. Pump reflection was used because the performance of OPOs using nonlinear crystals with relatively low effective nonlinearity benefits strongly from double-pass pumping. Furthermore, two-pass pumping ensures collinear operation even without walk-off compensating crystals [6]. The idler wavelengths, in the 2-3 µm range for the experiments in discussion, were outside the range of the half-wave plate, both in terms of optical transmission and retardation, but they still experienced about 70% transmission and about a half-wave retardation. As shall be seen in Subsection 3.4, the performance of the OPO may still be affected by the half-wave plate because the relative phase of the interacting waves can be changed owing to dispersion of the optical thickness of the half-wave plate.

The crystal lengths, output couplings, and maximum pump energy for each pump beam diameter were determined through extensive simulations using FFI's simulation tool that accounts for all relevant effects [7, 8]. The optimal crystal lengths were found to be 2 × 30 mm KTP for the 1064 nm pumped OPO and 2 × 16 mm BBO for the 532 nm pumped OPO. The main reason for the shorter crystals at the shorter pump wavelength is that the nonlinear optical gain increases with frequency.

3. Results

3.1 Orthogonal vs. parallel critical planes

For a collinear $\chi^{(2)}$ interaction not along one of the crystal axes, there is in general a critical plane, where the phase mismatch varies rapidly with beam direction, and an orthogonal noncritical plane where it does not vary to first order. The OPO with parallel critical planes is equivalent to using one crystal with length equal to the sum of the two crystals, or to a pair of walk-off compensating crystals. The case of orthogonal critical planes (OCP) has the same overall gain; however, the half-wave plate rotates the polarization (but not the image) of the signal and pump beams between the crystals by 90°, thereby creating spatial coherence in both transversal directions [3].

Figure 2 shows the measured near and far fields of the 1680 nm signal beam for both parallel and orthogonal critical planes from a 1064 nm pumped OPO using the KTP crystal pair specified in Table 1. The pump beam diameter was ~4 mm and the pump energy was 80 mJ in this experiment.

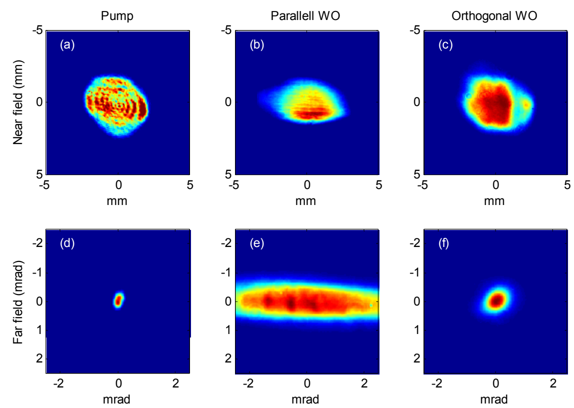

Fig. 2. Near (NF) and far fields (FF) for the 1064 nm pump and OPOs with KTP crystals oriented with parallel or orthogonal critical planes, and about 4 mm pump diameter. The OPO data were acquired at approximately 80 mJ pump energy, corresponding to around 20 mJ pulses at 1680 nm; NF of (a) pump, the case of (b) parallel and (c) orthogonal walk-off planes, FF of (d) pump, the case of (e) parallel and (f) orthogonal walk-off planes.

As expected (and explained above), the far field in the case of OCP is narrowed by the signal acceptance angle in both directions, giving a substantial improvement in beam quality. The output signal pulse energy as function of pump pulse energy is similar for the two configurations, with marginally higher slope and threshold for the case of orthogonal walk-off planes, leading to slightly higher conversion efficiency.

3.2 Pump diameter implication on beam quality

The basic idea of this work, as well as other work described in Section 1, is to use a narrow signal beam acceptance angle to restrict the divergence of the generated beams in an OPO with wide beams. One consequence of this technique is that the size of the far field stays about the same even if the pump diameter is increased, at comparable fluence levels. The beam quality (M^2) therefore increases linearly with the pump diameter; however, it is always much better than in OPOs with comparable beam diameters, but without the far field limiting methods described here [3]. The output signal pulse energy is plotted as function of pump pulse energy and compared for different pump beam diameters in Fig. 3 for the same OPO as described in Subsection 3.1.

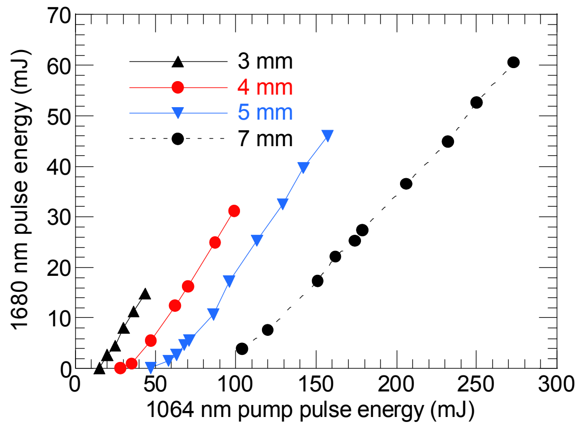

Fig. 3. Signal pulse energy as function of 1064 nm pump pulse energy for KTP OPO with orthogonal critical planes for 3, 4, 5 and 7 mm pump diameter (in terms of 90% energy in bucket).

The slope efficiency is nearly constant, but the threshold pump energy increases with increasing pump beam size. The reduction in slope efficiency for the largest pump beam is due to losses in the limited aperture available in the experiments (slightly below 8 mm × 8 mm). The measured far fields of the signal generated with different pump beam diameters, but at approximately the same pump fluence level (approximately 0.5 J/cm^2), are shown in Fig. 4. We notice that the divergence remains nearly constant, even if the near field diameter changes.

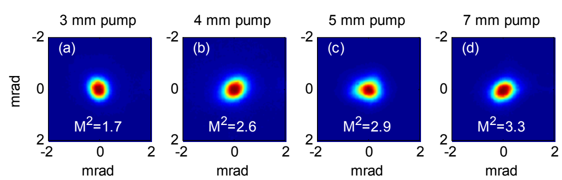

Fig. 4. 1680 nm signal far fields of the 1064 nm pumped OPO with orthogonal critical planes measured for 3 mm to 7 mm pump beam diameters as specified above each image, from (a) smallest to (d) widest pump beam at 25, 62, 96 and 174 mJ pump energy, respectively. The signal far fields are independent of pump beam diameter. The near fields of the signal were approximately 20% narrower than those of the corresponding pump.

3.3 Idler absorption implication on beam quality

The output wavelength of a 532 nm pumped OCP OPO using the BBO crystal pair was varied by angle tuning the BBO crystals (around orthogonal rotation axes). While the nonlinear coupling coefficient is nearly constant at the three wavelengths, the absorption at the idler wavelength varies greatly in BBO. Table 2 lists the idler wavelengths and corresponding absorption.

Table 2. Idler Characteristics at Different Signal Wavelengths[b]

Signal wavelength	Idler wavelength	Idler absorption	Tuning angle
650 nm	2930 nm	283 m^{-1}	23.1°
670 nm	2580 nm	105 m^{-1}	23.6°
720 nm	2037 nm	7 m^{-1}	25.0°

[b]Idler wavelengths and corresponding BBO tuning angles and idler absorption coefficients for signal wavelengths used in Subsection 3.3 [9].

We have previously shown through simulations that at low pulse rates idler absorption may be beneficial for the performance of an OPO [1], as removal of idler prevents detrimental back conversion and makes it possible to operate the OPO at a higher pumping level. Figure 5 shows the output energy as function of the pump energy for the three different wavelengths as well as the beam quality expressed as M^2. Interestingly, increasing the idler absorption from weak (7 m^{-1}) to strong (105 m^{-1} which corresponds to 3.5% single pass transmission) does not affect the output energy from the OPO in a significant manner, but helps to improve the beam quality. This confirms the findings in [1], and originates from less back conversion with higher idler absorption. On the other hand, moving to very strong idler absorption (283 m^{-1}) improves the beam quality further, but at the expense of reduced output energy.

The experiments were carried out using only a 3 mm wide pump beam due to a mechanical damage on one of the BBO crystal faces. We expect a more pronounced effect using a wider pump beam and higher pump energies. During initial experiments, 70-75 mJ of output energy at 670-720 nm was obtained when pumping with 170 mJ in a ~7 mm diameter pump beam.

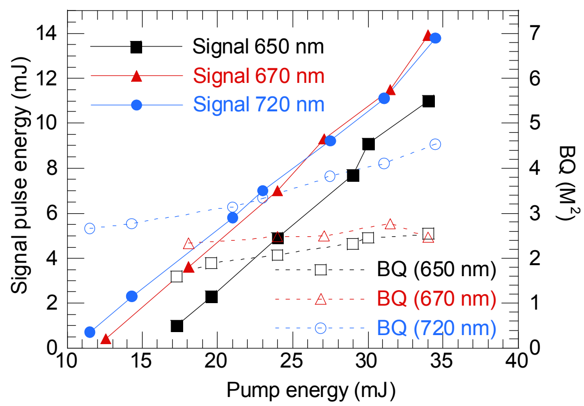

Fig. 5. Measured signal energies (left hand axis) and beam quality (right hand axis) at 650 nm, 670 nm and 720 nm signal wavelengths, corresponding to 283 m^{-1}, 105 m^{-1} and 7 m^{-1} idler absorption in BBO, respectively. The pump beam diameter was approximately 3 mm.

3.4 Effect of relative phase shift in half-wave plate

The different optical thickness of the half-wave plate at the pump, signal and idler wavelengths will result in a shift in the relative phase of the three beams. This may have significant effect on the OPO performance [10, 11], and was studied through simulations. Figure 6 shows the simulated performance of the 1064 nm pumped KTP OPO as function of relative phase shift. It is clear that the signal energy and signal beam quality are strongly affected by this, in particular when the phase shift approaches a half-wave (π).

#192125 - $15.00 USD Received 17 Jun 2013; accepted 16 Jul 2013; published 20 Aug 2013

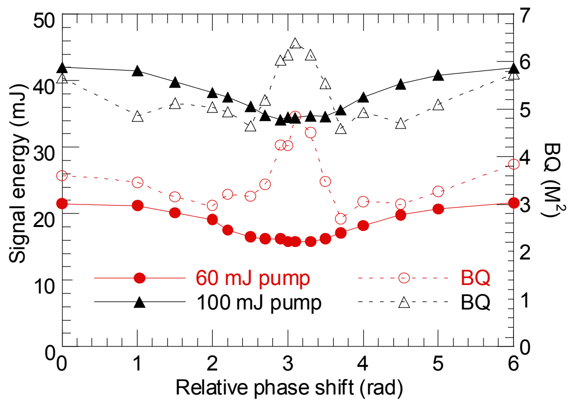

Fig. 6. Simulated performance of a 1064 nm pumped KTP OPO as function of relative phase shift through the half-wave plate. In the simulations, 60 and 100 mJ pump energy in a 4 mm diameter beam were assumed along with the experimental parameters listed in Section 2.

The signal energy is reduced by ~25% in this case when the phase shift is increased from 0 to 2.5 rad, without a reduction in beam quality. However, if the phase shift is further increased towards π, the beam quality is significantly reduced. This happens because the OPO adapts to the phase shift by running on two noncollinear signal modes, as shown in Fig. 7.

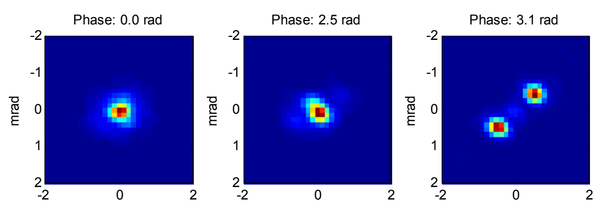

Fig. 7. Far field of simulated KTP OPOs in Fig. 6 at different relative phase shifts.

It was not within the scope of this work to measure the phase shift. However, simulations of the OPO performance show good agreement with experiments when the relative phase shift is about 2.5. In particular, the splitting of the far-field was not observed in the experiment. Figure 8 shows a comparison between experimental results and simulations for 0 and 2.5 rad phase shift for 4 mm pump diameter.

#192125 - $15.00 USD Received 17 Jun 2013; accepted 16 Jul 2013; published 20 Aug 2013

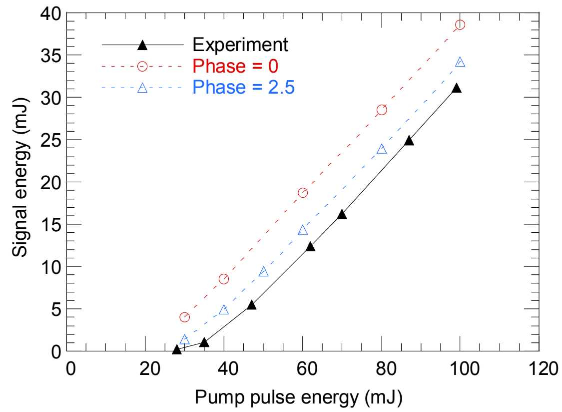

Fig. 8. Comparison of experimental data and simulations for a 1064 nm pumped KTP OPO with 4 mm diameter pump beam. The simulations are for 0 and 2.5 rad relative phase shift in the half-wave plate.

4. Conclusion

The divergence of high-pulse-energy, nanosecond OPOs using type 2 critical phase matching is restricted by the acceptance angle in the walk-off plane. This gives an asymmetric beam quality as long as the crystals in the same cavity are oriented with parallel walk-off planes. However, if two identical crystals oriented with orthogonal walk-off planes are used in the same resonator, and the polarizations of the interacting beams are rotated by 90° (by an achromatic wave plate) between the crystals, the divergence is restricted in both transversal directions, resulting in a symmetric beam with greatly improved beam quality. Two-pass pumping not only increases conversion efficiency, but also consolidates collinear phase matched operation. We have demonstrated this principle by generating a symmetrical beam with pulse energies exceeding 60 mJ at 1680 nm from an OPO with two KTP-crystals, when pumped with 5 ns pulses from a 1064 nm Nd:YAG laser. The same geometry using BBO-crystals was also used to convert 532 nm pulses to 75 mJ pulses in the red. The OPO is easily tunable, and signal wavelengths in the range from 650 nm to 720 nm were demonstrated for the purpose of varying idler absorption in BBO from 283 m^{-1} to 7 m^{-1}. At the 10 Hz pulse rate used in this work, OPOs with high idler absorption perform better than OPOs with low idler absorption, in support of previous simulation results [1]. This is explained by less back conversion in the case of high idler absorption. The relative phase shift induced by the half-wave plate may have substantial effect on the performance of the OPO in terms of conversion efficiency and beam quality, as predicted by simulations. A relative phase shift close to a half-wave should be avoided, since this forces the OPO to run noncollinearly, splitting the far field in two distinct lobes and reducing the beam quality.

Acknowledgments

The authors would like to acknowledge Gunnar Arisholm and Knut Stenersen, FFI, for valuable comments and discussions concerning the manuscript.